

Section VII

Plasmas and Fields

The Magnetic Field Structure of the Cometary Plasma Environment

F. M. Neubauer

Institut für Geophysik und Meteorologie, Universität Köln

Albertus-Magnus-Platz

5000 Köln 41

FRG

ABSTRACT. The plasma surrounding a comet has the interplanetary magnetic field frozen in. The geometric interpretation of this property is considered. The frozen-in character of the magnetic field leads to the draping of magnetic field lines around the inner coma, where, by exclusion of the inner purely cometary ionosphere, a magnetic cavity is formed inside a region of magnetic field pile-up. The consequences of these physical processes can nicely be diagnosed and tested by interplanetary tangential discontinuities serving as tracers of the magnetoplasma flow. The topology of the magnetic field around the cavity and the shape of the ionopause, as well as the formation of the magnetic tail, are discussed. Particularly in the outer regions, the magnetic field is disturbed by strong magnetic turbulence. This turbulence plays a role in accelerating cometary and also solar wind ions to high energies.

1. Introduction

The essential physical feature of the interaction between a cometary atmosphere and the solar wind is the assimilation of newly created cometary ions into the overall plasma flow, which, far from the cometary nucleus, is dominated by plasma of solar origin flowing radially from the sun and, closer to the comet is more and more dominated by cometary ions. The creation of cometary ions is mainly due to photoionization of cometary neutrals, but collisional processes also play a role. In the first study of the comet solar wind interaction, i.e., in the pioneering paper by Biermann (1951), the interaction between newly created cometary ions and the plasma flow was attributed to Coulomb collisions. The low efficiency of momentum coupling due to Coulomb collisions led to estimates of the solar wind densities several orders of magnitude too high, as we know today. A much more efficient process to couple the various charged particle species is the coupling by the plasma magnetic field first realized by Alfvén (1957) in cometary physics. This can be made more quantitative by considering the equation of motion for charged particle species i described by

$$\begin{aligned} \frac{d\mathbf{v}_i}{dt} = & -\frac{1}{\rho_i} \text{grad } p_i - \frac{1}{\rho_i} \nabla \cdot \underline{\tau}_i + \frac{Q_i}{m_i} \underline{E} + \mathbf{v}_i \times \underline{\Omega}_i \\ & + \sum_{j=i} \nu_{ij} (\mathbf{v}_j - \mathbf{v}_i) + \frac{q_i}{n_i} (\mathbf{v}_n - \mathbf{v}_i) \end{aligned} \quad (1)$$

with n_i , $\rho_i = n_i m_i$, \mathbf{v}_i and p_i being the number density, mass density, velocity vector and pressure of the species i , respectively. $\underline{\tau}_i$ is the stress tensor. The charged particle species i has the

charge Q_i and mass m_i . Ω_i is the signed cyclotron frequency vector $\Omega_i = \frac{Q_i}{m_i} \underline{B}$, with \underline{B} being the magnetic field. \underline{E} is the electric field. ν_{ij} is the Coulomb collision frequency between species i and j . q_i is the volume production rate of species i , and \underline{v}_n the neutral gas velocity of the neutral parents. The addition of collisions between neutrals and charged particle species leads to terms analogous to the last term on the right-hand side of equation 1. We see from equation 1 that the ratio of the Lorentz force term to the collision terms involving \underline{v}_i and the similar particle production term is given by

$$R_i = \frac{\Omega_i}{\sum_{j \neq i} \nu_{ij} + q_i/n_i} \tag{2}$$

This ratio R_i turns out to be > 1 throughout the cometary interaction region. For a comet like P/Halley near 1 AU, the ratio decreases from large values far from the comet to smaller and smaller values, until in the magnetic field cavity, with $B = 0$, the ratio drops to zero.

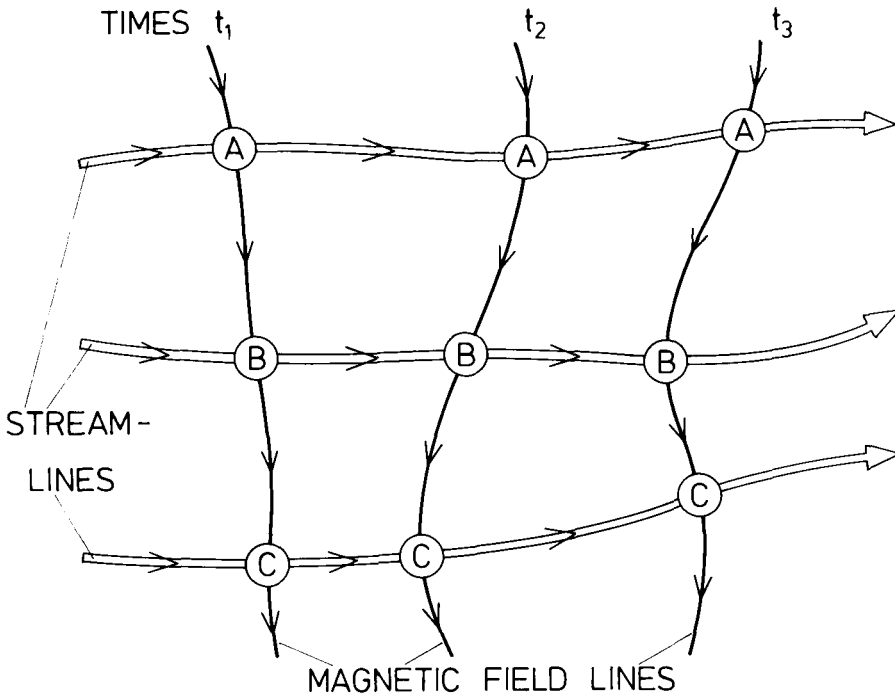


Figure 1. Sketch illustrating the frozen-in-field concept. If particles A,B,C,... are located on a fieldline at time t_1 , they will always be located on one field line at a given time t_2 or t_3 or t_4 etc. Streamlines describe the motion in the velocity field \underline{u} .

The condition $R_i \gg 1$ is a necessary condition for the frozen-in-magnetic-field theorem to be valid. This theorem can be stated as follows

$$\frac{\partial \underline{B}}{\partial t} = \text{rot} (\underline{u} \times \underline{B}) \tag{3}$$

where \underline{u} is a velocity defined as

$$\underline{u} = \sum_{\text{ions}} n_i \underline{v}_i / n \tag{4}$$

with the total charged particle density $n = \sum_{\text{ions}} n_i$. Additional conditions for the validity of equation 3 are spatial and temporal scales greater than the largest thermal gyro radius and the largest ion cyclotron period, respectively.

The formulation involving equations 3 and 4 is due to Marochnik (1982), who has shown that in the cometary case, \underline{u} must be used instead of the bulk velocity \underline{v} , which is mass weighted

$$\underline{v} = \sum \rho_i \underline{v}_i / \rho \tag{5}$$

with the total mass density $\rho = \sum \rho_i$. Equation 3 describes the close coupling of the flow characteristics in \underline{u} and the magnetic field. One of the most important geometric interpretations of equation 3 is illustrated in Figure 1. Plasma elements moving with velocity \underline{u} (in contrast to mass elements moving with the bulk velocity \underline{v}) have the following property: If plasma elements A, B, C, ... are positioned on one field line at time t_1 , they are positioned on the same field line at any other time. The frozen-in-field concept is the basis for the concept of field line draping to be considered in the next section. The frozen-in-field concept constitutes an important tool to develop the overall topology of a plasma flow system to which it can be applied, to visualize the complex flow characteristics and to diagnose a plasma flow. Part of the usefulness of this concept stems from the fact that $\text{div} \underline{B} = 0$, i. e., that magnetic field lines cannot have open ends and must remain intact whenever equation 3 is fulfilled.

Under the conditions of strong validity of the frozen-in-field theorem, the charged particle distribution functions are approximately gyrotropic in a common frame of reference moving with $(\underline{E} \times \underline{B})/B^2$. In this case, the chemical and kinetic properties of the particles can vary appreciably perpendicular to the magnetic field, but only weakly parallel to the magnetic field.

The momentum budget of the bulk flow is determined by three contributions. The first two are the pressure gradient force and the magnetic field force per volume given by

$$\underline{F}_p = -\text{grad } p - \text{grad } \underline{\tau} \tag{6a}$$

$$\underline{F}_m = \underline{j} \times \underline{B} \tag{6b}$$

where $p = \sum p_i$, \underline{j} is the current density and $\underline{\tau} = \sum \underline{\tau}_i$. The third force \underline{F}_c due to the addition of momentum by the creation of new cometary ions and neutral-charged particle collisions is not given in detail here. The relative importance of \underline{F}_p and \underline{F}_m is given by the plasma β value

$$\beta = p / \frac{B^2}{2\mu_0} \tag{7}$$

i.e., the ratio of plasma to magnetic field pressure. β grows slowly with distance from the sun in the solar wind far from the comet apart from dynamical variations. Near 1 AU, β is typically 1. Here, the plasma is dominated by the forces \underline{F}_p and \underline{F}_m on an equal basis. As the comet is approached, β grows, due to the increasing density and plasma temperature.

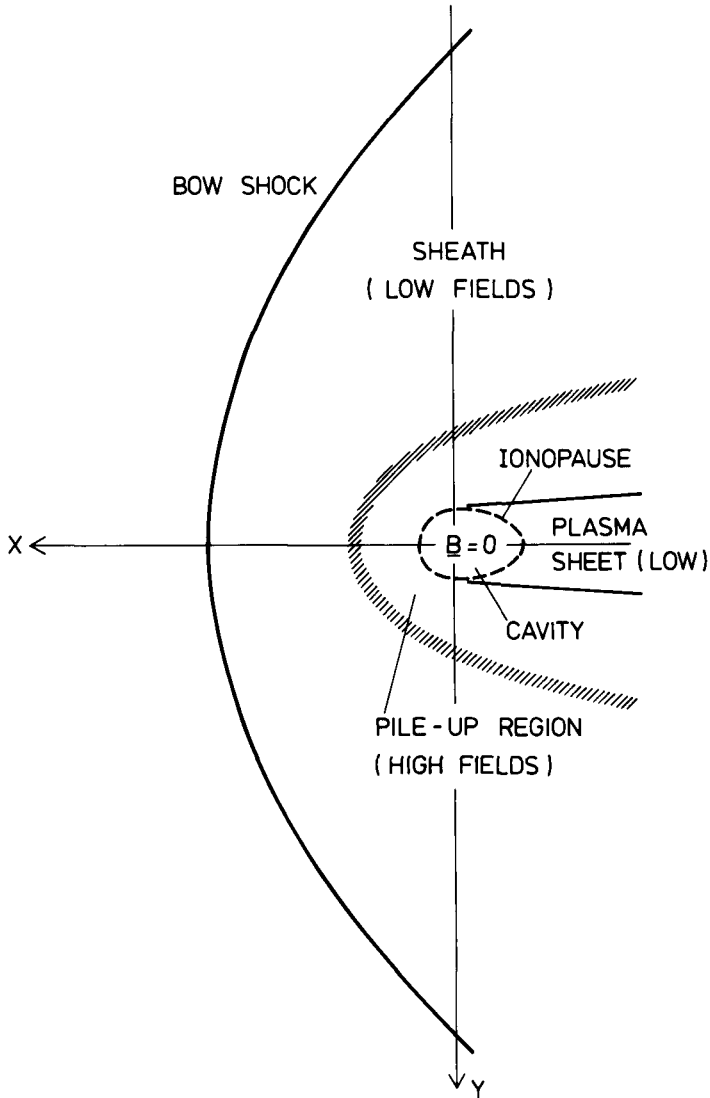


Figure 2. Sketch illustrating boundaries in the magnetic field around a comet. The most consistent discontinuity boundaries are the bow shock and the ionopause, i.e., the boundary of the magnetic cavity. The boundary between the low and high magnetic field regions, which varies in nature, is shown by cross-hatching. For better visibility, the size of the cavity is shown highly exaggerated.

Although the magnetic field does not contribute much to the momentum balance far from the comet, it is important in shaping the distribution functions and therefore the stress terms $\underline{\tau}$. Close to the comet, β decreases well below 1, although the lack of a full set of plasma data in the inner coma prevents us from assigning a value to β just outside the cavity boundary. In the innermost part of the high magnetic field region, \underline{E}_m and \underline{E}_c are thought by several authors (Ip and Axford, 1987; Cravens, 1986) to balance each other. Inside the cavity $\beta \approx \infty$.

As in most problems of space plasma physics the cometary plasma is divided into several spatial regions by discontinuities, i.e., sheet-like regions in which strong gradients occur in at least some of the physical quantities. We give the cometary bow shock as one example and the ionopause, i.e., the boundary of the cavity, as another example. In the magnetic field, these cometary discontinuities occur very clearly. A schematic picture is shown in [Figure 2](#). A three-dimensional perspective view can be found in Neubauer (1989). Many more discontinuities are seen in the observations; some of these discontinuities are of solar wind origin and some may be connected with the cometary plasma physics but exist only temporarily. In magnetohydrodynamics, five types of discontinuities are allowed, in contrast to only two in gasdynamics. An important task in the analysis of in situ plasma observations is to determine not only the location of a discontinuity crossing but also the local discontinuity normal \underline{n} . In many cases, this can be done by using a so-called minimum variance analysis (MVA). The MVA (Sonnerup and Cahill, 1968) searches for that direction which has the smallest component variance. From $\text{div} \underline{B} = 0$, it follows that for any one-dimensional structure varying only in the \underline{n} -direction, $\underline{B} \cdot \underline{n} = B_n$ must be constant. This property is used to find \underline{n} .

Before we start the detailed discussion of the magnetic field in the cometary plasma environment, it is worth mentioning the magnetic field's role for charged particles as a function of energy. Charged particles typical for the bulk of the plasma experience forces due to the electric field, magnetic field, Coulomb collisions and collisions with neutral particles. A high-energy charged particle "sees" the comet as a magnetic structure with some role also played by collisions with the neutral gas very close to the comet.

2. Macroscopic Magnetic Field Structure

The magnetic fields observed by spacecraft or from the ground in the cometary environment are due to the distortion of interplanetary field lines by the plasma flow near the comet. The roots of these field lines are finally to be found in the sun.

Small internal magnetic fields can be expected in and near the cometary nucleus due to a natural remanent magnetization of suitable mineral components, such as magnetite, in the cometary dust. This field is expected to be observable in the near vicinity of the cometary nucleus only, however.

The interplanetary magnetic field of solar origin is carried outward by the solar wind flow and follows Archimedean spirals wrapped on cones around the rotation axis of the sun at constant heliographic latitude λ_o . For a solar angular rotation rate Ω_o and a mean solar wind velocity $V_{s,o}$ the angle between \underline{B} and the radial direction is given by ϕ with

$$\tan \phi = \frac{\Omega_o \cdot r_o \cos \lambda_o}{V_{s,o}} \quad (8)$$

where r_o is the radial distance from the sun.

For an average solar wind velocity, ϕ happens to be 45° or 135° near 1 AU, depending on polarity. Observations show a clustering of ϕ -values around the nominal values 45° and 135° . We shall return to this point in the next section.

For the solar wind velocity incident on the comet, we have to take into account the aberration due to the orbital motion of the comet. For the plasma interaction, the angle α between the magnetic field and the solar wind velocity \underline{v}_s in the frame of reference of the comet is important. Prograde cometary orbits push α away from 90° , and retrograde orbits toward 90° , as in the case of Halley's comet.

The solar wind flow incident on a cometary neutral atmosphere will be slowed down near the comet due to the mass loading. The mass loading rate per volume is a function of radial distance r from the nucleus, given in its simplest form by the photoionization rate, which, under optically thin conditions, is given by

$$q_m = m_i n_n / \tau_i \quad (9)$$

where m_i is the mass of a typical cometary ion, τ_i the photoionization lifetime due to solar radiation and $n_n(r)$ the neutral gas density given by a Haser model, for example. The slowing down of the solar wind is, at first, of minor importance. When the sonic Mach number has reached a value near 2 on the stagnation stream line, i.e., the stream line separating the stream lines diverted around the comet towards opposite directions, a bow shock forms. Inside the bow shock, the deceleration of the flow becomes more and more important until the velocity of the plasma flow becomes almost stagnant. The Giotto spacecraft, which approached the comet most closely, detected this region of plasma with $v_r \approx 0$ outside 4660 km from the cometary nucleus on the inbound Giotto trajectory. Whereas the flow aspects are treated in some detail in the articles by Flammer and by Cravens in this book we shall here concentrate on the magnetic field. [Figure 3](#) shows the magnetic field lines computed from the Schmidt and Wegmann model (Hübner et al, 1989) for an initial field angle of $\alpha = 57^\circ$ in the plane x, y spanned by \underline{v}_s and the initial magnetic field \underline{B} . The field line is frozen into the solar wind plasma, which is contaminated increasingly by cometary ions. The field line carried by the plasma is shown at times $t_F = 0, 5$ minutes, 10 minutes, etc. Because of the deceleration, which is largest on the central stream line (not shown), the central part of a field line lags behind those parts on the flanks. This explains the general behavior. The field line is shown until 170 minutes after it entered the denser parts of the cometary atmosphere more or less undistorted. The field line is wrapped increasingly around the inner region. This process, called field line draping, continues until, after a long time, an innermost position is reached. The innermost field lines define the outer boundaries of a region not reached by field lines of solar origin. The magnetic field in this region is essentially zero because of the extremely small field generated in the cometary nucleus. The region avoided by the solar magnetic field is called the magnetic cavity. One can define the boundary of the cavity as the boundary between external plasma, which is partly of cometary and partly of solar origin, and internal plasma, which is purely of cometary origin. This is except for a very small diffusive flux of solar protons and alpha particles through the ionopause and from the tail. In the inner 10^5 km at comet Halley observed by the VEGA and Giotto spacecrafts, the magnetic field has been piled up to magnitudes up to ten times the solar wind magnetic field. The curvature force of the magnetic field pulls the plasma towards the comet against the frictional force due to the neutral gas flow, etc., down to distances that would otherwise not be reached. Whereas the VEGA spacecrafts showed a gradual transition in the magnetic field from the outer regions inside the bow shock to the pile-up region (Riedler et al., 1986), Giotto observed a very sharp transition at the inbound pile-up boundary (Neubauer et al., 1986).

The discussion shows that the magnetic field in a stationary interaction problem can be obtained by following an initially undistorted field line as it is carried along frozen to the flow. The full three-dimensional field configuration can be obtained by picking initial field lines in several planes $Z = \text{constant}$.

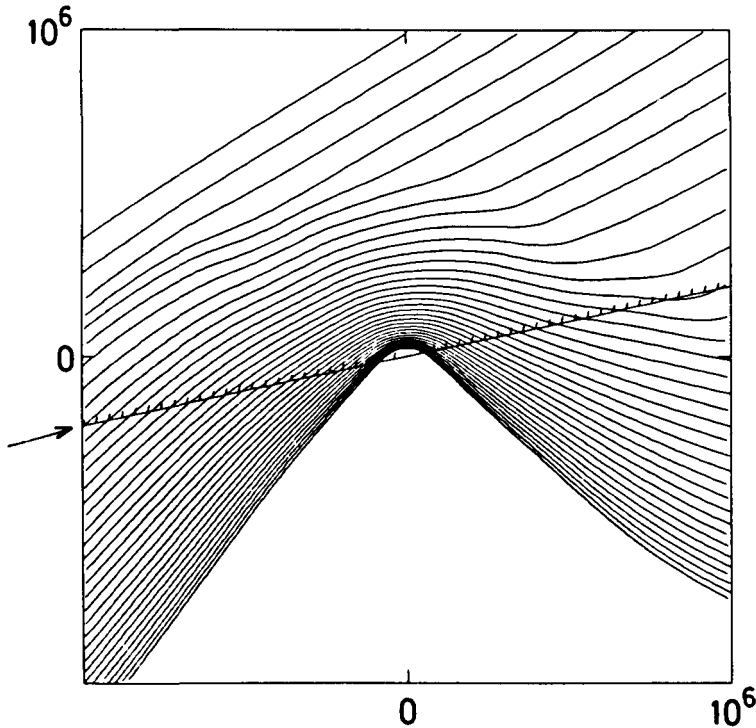


Figure 3. A frozen-in-field line convected towards the comet in the X, Y - plane shown at time increments of 5 minutes after Hübner et al. (1989) with the initial field line at upper left. X is pointing to the top and Y to the left of the figure. The velocity field has been taken from a cometary 3-D model simulating plasma conditions during the Giotto encounter. The Giotto trajectory is shown with tick marks ten minutes apart.

3. Interplanetary Discontinuities Used as Tracers in the Cometary Magnetoplasma

The frozen-in-field theorem applied to interplanetary tangential discontinuities (TDs) can be used for sensitive tests of the kinematics of the cometary plasma flow and therefore also for the testing of numerical models. This is because TDs are moving with the plasma.

Tangential discontinuities constitute a frequent type of discontinuity in the solar wind and other applications in space plasma physics. As one of the five types of magnetohydrodynamic (MHD) discontinuities, they are characterised by conservation of total pressure $p_t = p + B^2/2\mu_0$ across the tangential discontinuity and a vanishing component of the magnetic field and the plasma flow in the rest frame of the TD in the direction of the TD normal. Apart from stability problems, all other changes across the TD are arbitrary. Because of these characteristics, the magnetic field is always

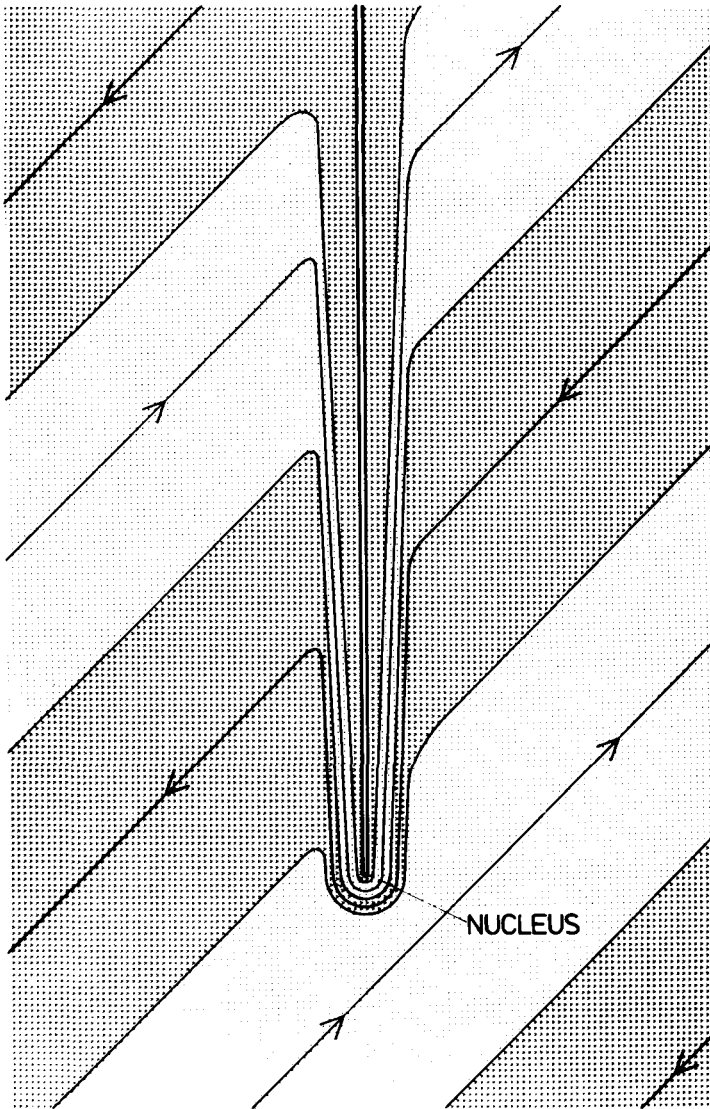


Figure 4. Schematic view of the flow distortions experienced by idealized sector boundaries draped around a comet.

parallel to a TD surface which is carried by the plasma without any relative motion. Because of the latter property, a parcel of plasma located at the TD at one time is always fixed to the TD on the same side. This property can be used to employ TDs as tracers of plasma flow.

A particularly useful type of TD is characterized by a change in magnetic field direction by 180° and no other change. Since arbitrary solutions to the equations of dissipationless MHD remain solutions if the magnetic field \underline{B} is replaced by $-\underline{B}$, the flow is not affected by an arbitrary number of tangential discontinuities of the latter type introduced into the plasma with the TD-surfaces formed by magnetic field lines. Adding dissipation, the situation changes, because the TD starts to evolve, thereby affecting the flow. In the cometary environment, collisional dissipation processes are expected to play a role only close to the comet. Another possibility is the occurrence of field line reconnection across a discontinuity. Reconnection at sector boundaries has been proposed as a mechanism for so-called tail disconnection events by Niedner et al. (1981).

Figure 4 gives a schematic view of the situation in the \underline{v}_s , \underline{B} - plane defined in front of the comet when a sequence of 180° - TDs is draped around the comet. The TD-surface which is initially a plane, is highly distorted by the draping. It is also seen that a suitable flyby orbit of a spacecraft could encounter the same TD several times.

The Giotto encounter occurred at a time when both the spacecraft and comet Halley were close to the so-called heliospheric current sheet. The heliospheric current sheet is a more or less warped surface at low heliographic latitudes separating a northern interplanetary magnetic field polarity hemisphere from the southern polarity hemisphere in a global view of the solar and interplanetary magnetic field. At the time of the Halley encounter, Giotto was located south of the current sheet most of the time, with some excursions to northern polarities. The southern polarity was outward from the sun at that epoch in the solar magnetic cycle. The heliospheric current sheet is also referred to as the magnetic sector boundary. Whereas in the ideal case, the sector boundary is a 180° - TD, in the real world, sector boundaries can be quite complicated transition regions from one polarity to the other. They are often associated with clusters of TDs with appreciable directional changes of the magnetic field. Comet Halley had just caught such a cluster of TDs when Giotto passed through its plasma environment.

Figure 5 shows observations of the magnetic field directions projected on the Halley-centered solar ecliptic (HSE) - X,Y - plane (Raeder et al., 1987). The strongest discontinuities in direction are successively denoted by the small letters i, h, g ... c, b, a as the comet is approached. During the outbound pass, the discontinuities are called A, B, C ..., i.e., capital letters are used. A one-to-one relationship between inbound and outbound discontinuities in the sense $a \hat{=} A$, $b \hat{=} B$, etc., is suggested by the data where the sense of polarity changes serves to order the discontinuities. The magnetic field characteristics suggest that they are TDs. The possible shape of some of the TDs is sketched in the figure. All this occurs at distances of less than 60000 km from the comet, where the TD's are convected relatively slowly through the cometary neighborhood.

Beyond the phenomenological approach in **Figure 5**, our picture of the processes involved can be tested by comparing the times of occurrence of the TDs with predictions by numerical models. This is done in **Figure 6** (Hübner et al., 1989). Using the model in **Figure 3**, one can assign the time t_F to every field line, i.e., the time travelled by a field line from the position of the first field line in the top left of **Figure 3**. t_F is a function of location only, i.e., $t_F = t_F(X,Y,Z)$. If t is the absolute observational time, then $t - t_F$ is the absolute time when a field line encountered by Giotto was located at the first field line position in **Figure 3**. $t - t_F$ therefore serves to identify a field line frozen into the plasma and carried towards the comet. **Figure 6** shows that for a given $t - t_F$, there is either one corresponding time t or three times t , i.e., a TD frozen into the plasma is observed once or three times, in principle. The discontinuity observations a, b, c ... are used to "calibrate"

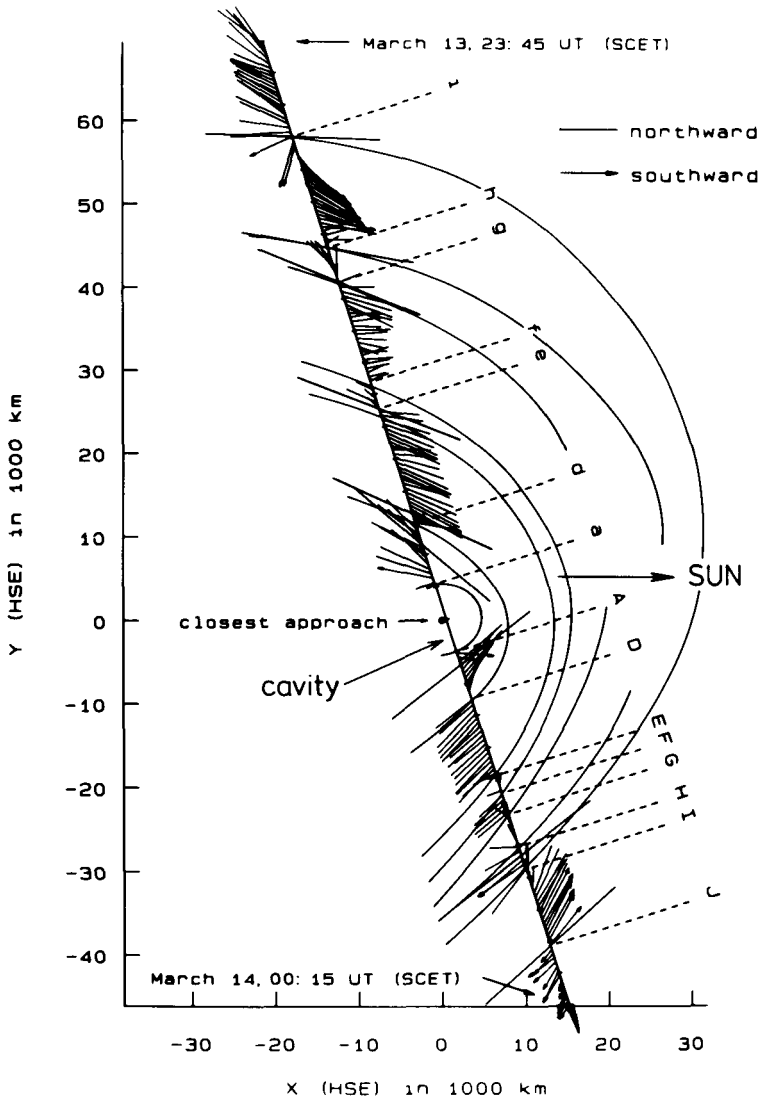


Figure 5. Observations of magnetic field directions along the Giotto trajectory from 23:45 UT SCET on March 13 to 00:15 UT on March 14 in the HSE X,Y - plane. The unit vectors based on 4-second averages and decimated by 2 have been projected on the X,Y-plane. Discontinuities are identified by lowercase letters before encounter and the corresponding ones by uppercase letters after encounter. The possible shape of the draped TDs is also shown, together with the cavity boundary.

the TDs by $t - t_F$. The figure then shows that the observations of the TDs A, B, C, D... agree with their predicted positions at intersections of the horizontal lines and the $t - t_F$ curve. The identification of the first expected crossings of the discontinuities is rather difficult because of the strong plasma turbulence at times more than 33 minutes before encounter. Altogether, this is a nice direct confirmation of the consequences of the frozen-in-field concept.

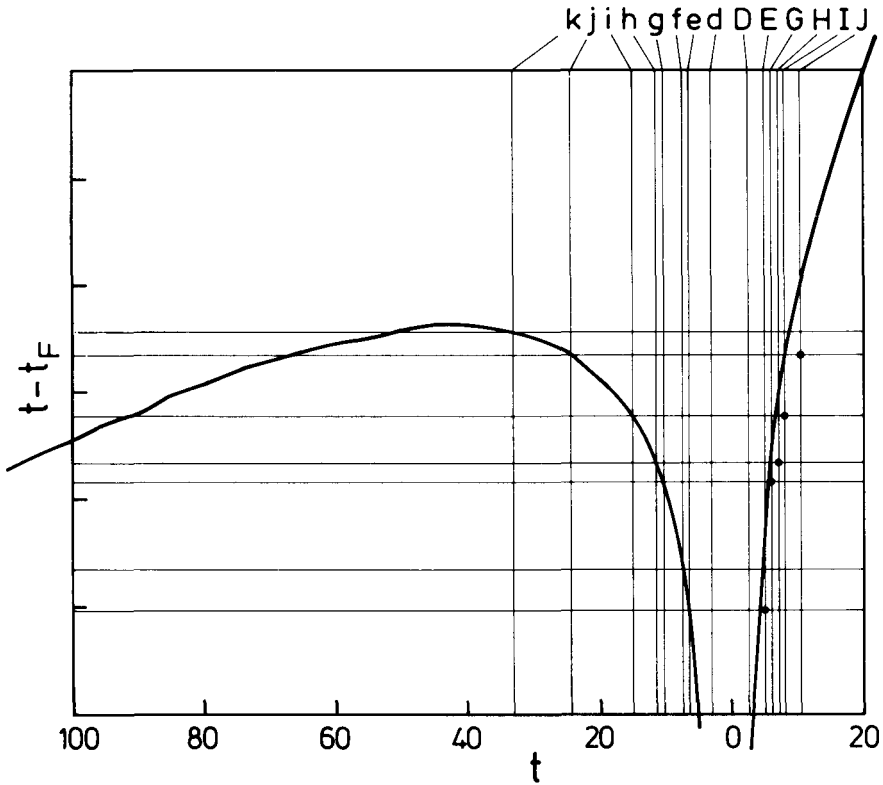


Figure 6. The time $t - t_F$ from the model by Hübner et al. (1989) as a function of time of observation t together with the locations of the TDs from Figure 5. For further discussion, see in the text.

4. The Magnetic Cavity and Tail Formation

We have already noted before that the innermost field lines draped around the comet define a spatial region devoid of a magnetic field, the magnetic cavity. The outer boundary of the cavity, the ionopause, is a sharp TD, as shown in Figure 7. The inward decrease of the magnetic field pressure at the ionopause is balanced by an excess plasma pressure just inside the ionopause in the cavity.

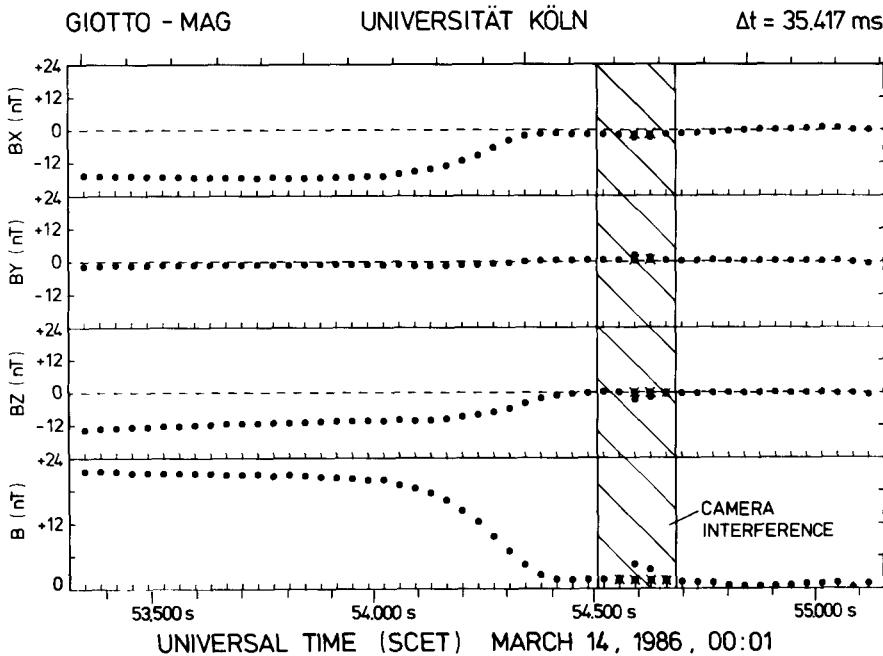


Figure 7. High time-resolution magnetic field observations of the inbound ionopause crossing of comet Halley by the Giotto magnetometer experiment.

A more detailed discussion of the plasma dynamics in this region is given in the article by Cravens in this book.

We are here particularly interested in the transition from the cavity on the tailward side to the cometary tail in the magnetic field topology. Insight can be gained by considering the motion of the field lines frozen into the cometary plasma. Field lines that have reached the cometary neighborhood at very small values of the Z -coordinate will move very slowly close to the X -axis and, because of the fast motion far from the X -axis, will be wrapped tightly around the inner coma region before they slip over the northern or southern part of the cavity boundary. These arguments indicate that the excessive draping deep in the pile-up region leads to a hairpin-like configuration which is largely independent of the angle α if only α is not too close to $\alpha = 0^\circ$. We take, therefore, $\alpha = 90^\circ$ to further develop the magnetic field topology just outside the ionopause and the ionopause shape itself. For $\alpha = 90^\circ$, the ionopause shape must be symmetric with respect to the X, Y - and X, Z - planes.

The distortion of a fieldline starting out at a long distance from the inner coma region at small $Z = +\epsilon$ is shown in [Figure 8](#) at consecutive times t_1, t_2, t_3, t_4 etc. In analogy to the discussion of

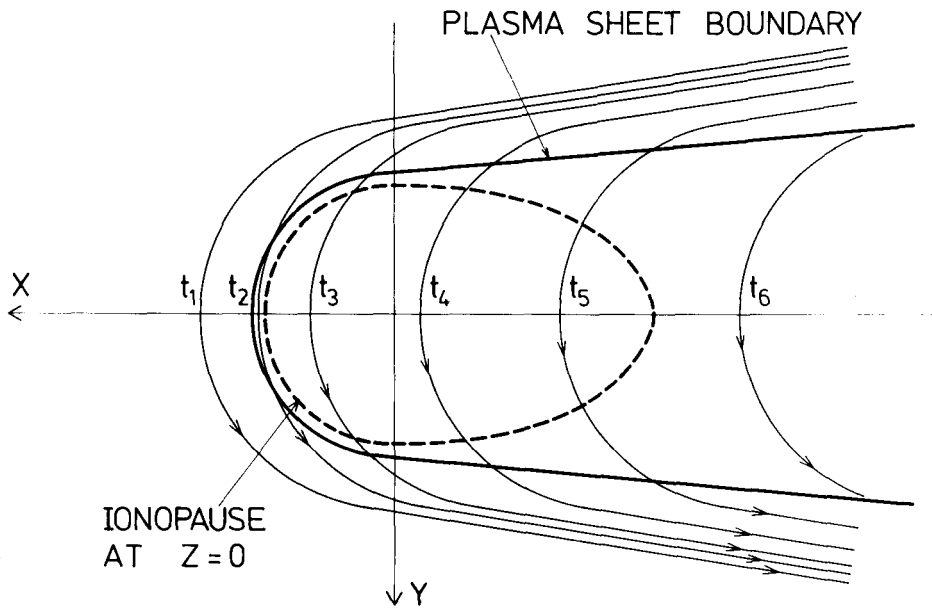


Figure 8. Draping of field lines around the cavity close to the nucleus in connection with the formation of the magnetic tail: A field line that has started with $Z > 0$ is shown at different times $t_1 < t_2 < t_3 < t_4 \dots$ projected on the X, Y - plane. The possible cavity shape is shown by a dashed line. For each field line the maximum Z occurs at $Y = 0$. The maximum Z for all times is expected at some time $t = t_4$, say.

Figure 3, the picture can also be understood as a snapshot showing several field lines at one time, e.g., t_1 . Figure 8 shows the projection of the field lines on the X, Y -plane. At all times, the highest value of Z on a fieldline occurs at $Y = 0$ because of the symmetry of the field lines. From this reasoning, it follows that the ionopause shape on the front side, i.e., at $X > 0$, must be spherical or elliptical. The tailward end of the cavity boundary is less simple. For a smooth descent of the field lines from maximum Z towards the asymptotic value $Z = \epsilon$ expected also at large values of $(-X)$, we deduce a cusp-type shape of the intersection with the X, Z - plane. A corner-type profile in this plane would require abrupt directional variations in the field lines at $|Y| \neq 0$, and therefore singularities in the pressure force and/or acceleration of the plasma for which there is no reason. The boundary could have the shape of a tadpole. No completely satisfactory self-consistent model is available for the ionopause shape yet, particularly on the tailward side. The self-consistent model of Schmidt et

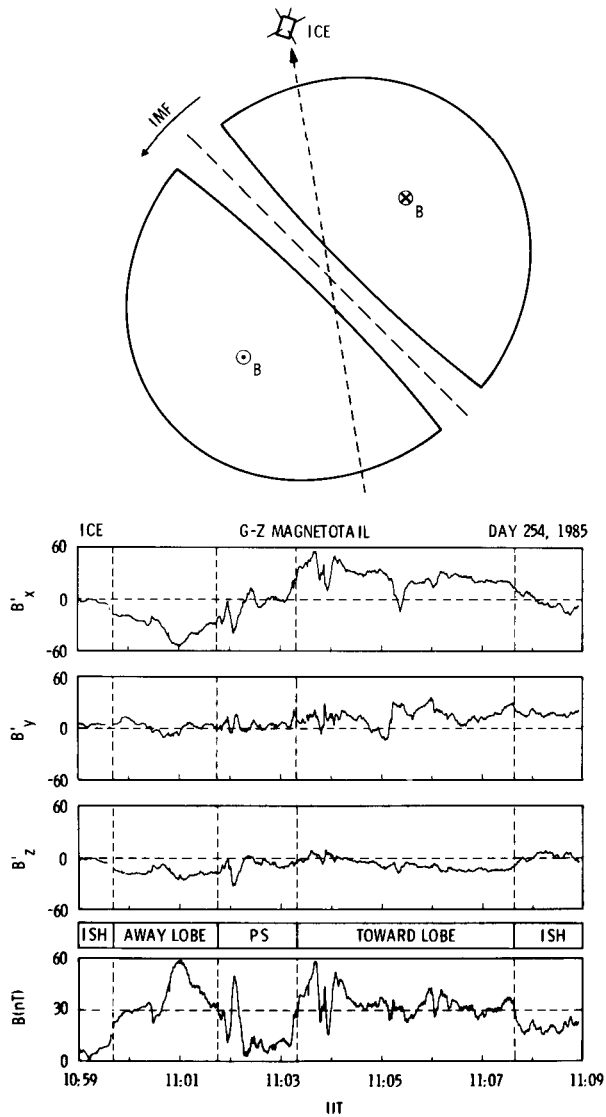


Figure 9. The magnetic field observations by the ICE spacecraft during the crossing of the tail of comet Giacobini-Zinner on September 11, 1985. High-resolution, 3 vector/second magnetic field observations are displayed in aberrated comet centered solar ecliptic coordinates for an interval containing the Giacobini-Zinner magnetotail traversal with the ionosheath, tail lobe, and plasma sheet region labelled. A schematic of the encounter geometry, viewed from behind the comet, looking sunward, is shown in the top panel (Slavin et al., 1986).

al. (1987) has not enough spatial resolution in this region. It indicates a distance from the nucleus to the tailward end of the ionopause of twice the subsolar distance. The model by Wu (1988) is not self-consistent in several respects. Observational evidence is provided by the Giacobini-Zinner (GZ) encounter data only. They show that, at the distance of about 7800 km, the cavity does not exist any more. This should be compared with an estimated subsolar distance of 600 km (Slavin et al., 1987). In the GZ plasma sheet, i.e., the region near $Y = 0$ where the X-component of the magnetic field changes sign, the magnetic field is small but different from zero in a relatively broad region, i.e., the curvature in the "hairpins" is relatively small and a neutral sheet does not exist. This is shown in [Figure 9](#) (Slavin et al., 1986).

Behind the tailward end of the cavity, the neutral gas-plasma interaction continues to decline such that the tensional force on the magnetic field lines can start to accelerate the plasma tailward. This is associated with a gradual opening of the "hairpins" far downstream of the comet.

5. Magnetic Turbulence

The picture of the comet solar wind interaction expressed in the magnetic field structure developed so far has been illustrated by field lines that look rather smooth in [Figures 3](#) and [4](#), for example. In reality, even when there is no evidence for solar wind disturbances convected or propagated into the cometary environment, there are strong irregular magnetic field variations superimposed on the draped macroscopic magnetic field (e.g., Tsurutani and Smith, 1986; Glassmeier et al., 1989). This is except for the region of magnetic field pile-up. The strong variations may be called loosely magnetic turbulence. This topic is treated in some detail in the accompanying articles by Galeev and Tsurutani in this book. Since the treatment of the magnetic structure of the cometary plasma environment would be incomplete without this aspect, we shall give here a brief overview.

The occurrence of electromagnetic instabilities relevant for cometary plasma physics was first recognized by Wu and Davidson (1972) for a magnetized plasma in which new ions are formed by the ionization of neutrals with a different bulk speed. In addition to the undisturbed initial plasma distribution, a ring-like distribution forms in velocity space with free energy that could at least partly go into magnetic turbulence. Although the instabilities have been known, the large amplitude of the generated nonlinear waves had not been predicted before the cometary encounters. The fluctuation amplitude sometimes almost reaches the average magnitude of the magnetic field.

The situation becomes even more complicated when solar wind disturbances are carried into the cometary plasma environment. TDs can again be used as evidence for the "contamination" of the cometary magnetic turbulence by interplanetary disturbances. This is because TDs are difficult to generate and to destroy. An interesting example is given by the magnetic field observed during the Giotto encounter. There is appreciable evidence for the occurrence of interplanetary disturbances during the inbound part of the flyby trajectory and the inner part of the outbound trajectory. A subdivision of the Giotto data into different regions of magnetic turbulence is given in [Figure 10](#). We take [Figure 10](#) as an example for the phenomenology of the magnetic turbulence region near a comet which is only partly understood at the time of this writing. The upper panel shows the magnetic field magnitude based on 64-second averages to illustrate the macroscopic magnetic field regions and the wave regions with the letters A, B, C... O corresponding to Glassmeier et al. (1987). The central panel shows the trace of the covariance spectrum based on 1-second averages for time intervals of 2048-second length computed with 30 degrees of freedom, and the lower panel, the normalized

Pythagorean mean component variance based on 1024-second intervals and 4-second averages with the linear trend removed. The figure shows the gradual increase of wave activity by large amounts as the distance to the comet decreases both inbound and outbound in the regions upstream from the comet's shock and foreshock regions.

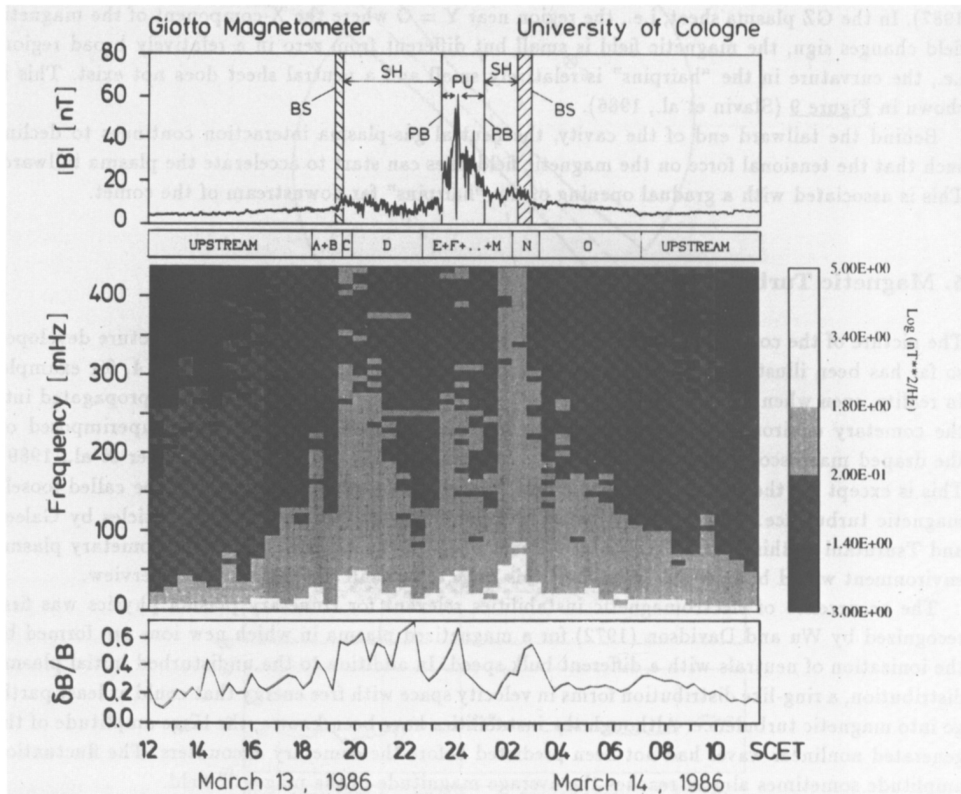


Figure 10. Magnetic turbulence in the vicinity of comet Halley, after Glassmeier et al. (1987). The upper panel fixes the relationship to the macroscopic plasma structure. The central panel shows the trace of the covariance spectrum of the magnetic field. The lower panel gives the Pythagorean mean component variances. For further details, see in the text.

Deviations from a smooth variation may be due to solar wind disturbances. We can identify a foreshock region A + B followed by the inbound bow shock region C followed by decreasing turbulence in region D. Regions E to M were characterized by distinct wave properties. The peak in wave intensity around midnight is partly due to higher-order trends and not to waves. N can be named the outbound shock region and O the outbound foreshock. In O, the waves have a trapezoidal shape, which is particularly noteworthy (Glassmeier et al., 1987). The figure shows that even in the normalized Pythagorean mean variances, the comet stands out clearly by $\delta B/B$ up to 0.6. In the spectra of the central panel, the comet is even more dramatic. For example, at $f = 50$

mHz, an increase of the trace spectral density by more than three orders of magnitude is observed. As already mentioned, the inbound regions A through J are affected by solar wind disturbances. Without these disturbances, the wave data would probably be close to symmetric around closest approach at 00:03:02 UT Spacecraft Event Time (SCET) on 14 March, 1986. Unexpectedly, the strongly nonlinear wave fields associated with comets Giacobini-Zinner and Halley have turned out to be a very exciting field of research for the plasma wave investigator. The magnetic turbulence produced by the pick-up of cometary ions has turned out to be very valuable as a diagnostic tool for cometary plasma processes. In addition, it serves as a means to accelerate a small part of the ion population to higher energies by means of Fermi acceleration and transit time damping.

6. Conclusions

In this article we have tried to develop a picture of the magnetic environment of a comet interacting with the solar wind. We have shown that an intimate coupling exists between the plasma and the magnetic field that expresses the importance of the magnetic field for the plasma dynamics and its diagnostics. Particular theory and spacecraft observations, but also some ground-based observations, have led to a picture that is generally understood in simple terms except for the formation of the tail, some aspects of the interaction with interplanetary disturbances and the physical mechanisms leading to the strong magnetic turbulence operative in comets. Here, both additional detailed observations and theoretical studies are necessary. We also indicated that comets can accelerate charged particles to high energies.

Acknowledgements: The author gratefully acknowledges the contributions by the experiment teams to the various magnetometer experiments and the support of observational and theoretical research by many financing agencies. This work was supported by the Bundesministerium für Forschung und Technologie of the FRG.

References

- Alfvén, H. (1957), 'On the theory of comet tails', *Tellus*, 9, 92-96.
- Biermann, L. (1951), 'Kometenschweife und Solare Korpuskularstrahlung', *Zs. f. Astrophysik*, 29, 274-286.
- Cravens, T.E. (1986), 'The physics of the cometary contact surface', *ESA SP-250, Volume I*, 241-246.
- Glassmeier, K.H., Coates, A.J., Acuna, M.H., Goldstein, M.L., Johnstone, A.D., Neubauer, F.M., and Reme, H. (1989), 'Spectral characteristics of low-frequency plasma turbulence upstream of comet p/Halley', *J. Geophys. Res.*, 94, 37-48.
- Glassmeier, K.H., Neubauer, F.M., Acuna, M.H., and Mariani, F. (1987), 'Strong hydromagnetic fluctuations in the comet P/Halley magnetosphere observed by the Giotto magnetic field experiment', *ESA SP-250, Volume III*, 167-171.
- Huebner, W.F., Boice, D.C., Schmidt, H.U., Schmidt-Voigt, M., Wegmann, R., Neubauer, F.M., and Slavin, J. (1989) 'Time-dependent study of magnetic fields in comets Giacobini-Zinner and Halley', *Adv. Space Res.*, Volume 9, No. 3, (3)385-(3)388.
- Ip, W.H., and Axford, W.I. (1987), 'The formation of a magnetic field free cavity at comet Halley', *Nature*, 325, 418-419.

- Marochnik, L.S. (1982) 'Solar wind magnetic field penetration into cometary ionospheres' *The Moon and the Planets*, D. Reidel Publishing Company, Dordrecht, pp. 353-370.
- Neubauer, F.M. (1989) 'Magnetic field regions formed by the interaction of the solar wind with comet Halley', in *Comet Halley, Investigations, Results, Interpretations*, Ellis Horwood Ltd., Chichester, England.
- Neubauer, F.M. (1988) 'The ionopause transition and boundary layers at comet Halley from Giotto magnetic field observations', *J. Geophys. Res.*, 93, 7272-7281.
- Neubauer, F.M., Glassmeier, K.H., Pohl, M., Raeder, J., Acuna, M.H., Burlaga, L.F., Ness, N.F., Musmann, G., Mariani, F., Wallis, M.K., Ungstrup, E., and Schmidt, H.U. (1986) 'First results from the Giotto magnetometer experiment at comet Halley', *Nature*, 321, 352-355.
- Niedner, M.B., Ionson, J.A., and Brandt, J.C. (1981) 'Interplanetary gas. XXVI. On the reconnection of magnetic fields in cometary ionospheres at interplanetary sector boundary crossings', *Astrophys. J.*, 245, 1159-1169.
- Raeder, J., Neubauer, F.M., Ness, N.F., and Burlaga, L.F. (1987) 'Macroscopic perturbations of the IMF by P/Halley as seen by the Giotto magnetometer', *Astron. Astrophys.*, 187, 61-64.
- Riedler, W., Schwingenschuh, K., Yeroshenko, Ye.G., Styashkin, V.A., and Russell, C.T. (1986) 'Magnetic field observations in comet Halley's coma', *Nature*, 321, 288-289.
- Schmidt, H.U., Wegmann, R., Huebner, W.F., and Boice, D.C. (1988) 'Cometary gas and plasma flow with detailed chemistry', Published in *Computer Phys. Comm.*, 49, 17.
- Slavin, J., Smith, E.J., Daly, P.W., Flammer, K.R., Gloeckner, G., Goldberg, B.A., McComas, D.J., Scarf, F.L., and Steinberg, J.L. (1987), 'The P/Giacobini-Zinner magnetotail', *ESA SP-250*, 81-87.
- Slavin, J.A., Smith, E.J., Tsurutani, B.T., Siscoe, G.L., Jones, D.E., and Mendis, D.A. (1986) 'Giacobini-Zinner magnetotail: ICE magnetic field observations', *Geophys. Res. Letts.*, 13, 283-286.
- Sonnerup, B.U.Ö, and Cahill, L.J., Jr. (1968), 'Explorer 12 observations of the magnetopause current layer', *J. Geophys. Res.*, 73, 1757-1770.
- Tsurutani, B.T., and Smith, E.J. (1986) 'Strong hydromagnetic turbulence associated with Comet Giacobini-Zinner', *Geophys. Res. Lett.*, 13, 259-262.
- Wu, Z.-J. (1988) 'Calculation of the shape of the contact surface at comet Halley', *Ann. Geophys.*, 6, 355-360.
- Wu, C.S., and Davidson, R.C. (1972) 'Electromagnetic instabilities produced by neutral particle ionization in interplanetary space', *J. Geophys. Res.*, 77, 5399-5406.